Taylor & Francis
Taylor & Francis Group

Artificial Cells, Nanomedicine, and Biotechnology
An International Journal

ISSN: 2169-1401 (Print) 2169-141X (Online) Journal homepage: informahealthcare.com/journals/ianb20

The efficacy of methylene blue encapsulated in silica nanoparticles compared to naked methylene blue for photodynamic applications

Ghaseb Naser Makhadmeh, Azlan Abdul Aziz & Khairunisak Abdul Razak

To cite this article: Ghaseb Naser Makhadmeh, Azlan Abdul Aziz & Khairunisak Abdul Razak (2016) The efficacy of methylene blue encapsulated in silica nanoparticles compared to naked methylene blue for photodynamic applications, Artificial Cells, Nanomedicine, and Biotechnology, 44:3, 1018-1022, DOI: 10.3109/21691401.2015.1008511

To link to this article: https://doi.org/10.3109/21691401.2015.1008511

Artificial Cells, Nanomedicine, and Biotechnology 2016; 44: 1018–1022

ISSN: 2169-1401 print / 2169-141X online
DOI: 10.3109/21691401.2015.1008511

Taylor & Francis
Taylor & Francis Group

The efficacy of methylene blue encapsulated in silica nanoparticles compared to naked methylene blue for photodynamic applications

Ghaseb Naser Makhadmeh[1,3], Azlan Abdul Aziz[1,3] & Khairunisak Abdul Razak[2,3]

[1]*Physics Department, School of Physics, Universiti Sains Malaysia, Penang, Malaysia,* [2]*Engineering Department, School of Materials and Mineral Resources Engineering, Universiti Sains Malaysia, Penang, Malaysia, and* [3]*NanoBiotechnology Research and Innovation (NanoBRI), Institute for Research in Molecular Medicine (INFORMM), Universiti Sains Malaysia, Penang, Malaysia*

Abstract

Background/Aims: **This study analyzed the physical effects of methylene blue (MB) encapsulated within silica nanoparticles (SiNPs) in photodynamic therapy.** ***Materials and methods:*** **The optimum concentration of MB needed to destroy red blood cells (RBCs) was determined, and the efficacy of encapsulated MB-SiNPs compared to that of naked MB was verified.** ***Results:*** **The results confirmed the applicability of MB encapsulated in SiNPs on RBCs, and established a relationship between the concentration of the SiNP-encapsulated MB and the time required to rupture 50% of the RBCs (t_{50}).** ***Conclusion:*** **The MB encapsulated in SiNPs exhibited higher efficacy compared to that of naked MB.**

Keywords: encapsulation, half-life time, methylene blue, photodynamic therapy, silica nanoparticles

Introduction

Photodynamic therapy (PDT) is a new cancer treatment that utilizes certain drugs that react with light. Exposing these drugs to light initiates a series of chemical reactions, to produce singlet oxygen, which leads to the destruction of cancer cells. However, the efficacy of singlet oxygen ($^1O_2$) production decreases considerably because a lesser amount of photosensitizer (PS) eventually reaches the intended target. The reduction in PS is attributable to the modification of the defense mechanism by the reticulo-endothelial system (RES) or the macrophage system, which engulfs some of the PS in the body. Nevertheless, the effect of macrophage cells is generally evaded by structures that are biocompatible and smaller than 100 nm, such as silica and gold nanoparticles. Based on this phenomenon, the efficacy issue associated with interactions with macrophages can be resolved using nanoparticles as a carrier for PS.

The high encapsulation efficiency of the silica nanoparticles (SiNPs) is due to their intrinsic properties. SiNPs exhibit high biocompatibility and low toxicity, which make them ideal material for a drug delivery system (DDS) (Bharali et al. 2005). Other intrinsic features of SiNPs include the ease with which they can be synthesized at low temperatures, with low polydispersity, the tendency for biomolecular compounds to adhere to their outer surface, and the ability of their inner surface to encapsulate the PS (Kneuer et al. 2000, Zhao et al. 2004, Santra et al. 2004).

The application of methylene blue (MB) (as a photosensitizer that will be encapsulated by SiNPs) in PDT is attributable to its low dark toxicity and high quantum yield of $^1O_2$ generation (Redmond and Gamlin 1999). Moreover, MB is also the least expensive of the commercially existing NIR fluorescent dyes, and has been overtly used for bioanalysis (Deng et al. 2006). Presently, intensive research studies are being carried out to harness the benefit of incorporating the fluorescence and photosensitivity of MB, to develop MB-encapsulated nanoparticle-based PDT (He et al. 2009). In this study, the applicability SiNP-encapsulated MB in PDT was demonstrated in an *in vitro* study using RBCs, because the RBCs are the vertebrate organism's principal means of delivering oxygen (O_2) to the body tissues via the blood flow through the circulatory system, and are also key players in transporting waste carbon dioxide from tissues to the lungs. Comparative analysis was performed between the efficacies of naked MB and encapsulated MB on RBCs, by studying their effectiveness at different concentrations and exposure times.

Materials and methods

Five different concentrations of MB (final concentrations of 2.50, 1.25, 0.63, 0.31 and 0.16 μM) were encapsulated within SiNPs. The synthesis of SiNP-encapsulated MB was achieved using the reverse-micellar method (Chatterjee et al. 2008). The dynamic light scattering (DLS) method was used to measure the dynamic size of the SiNP and its polydispersity when encapsulated with MB.

Correspondence: Ghaseb Naser Makhadmeh, School of Physics, Universiti Sains Malaysia, 11800 USM, Penang, Malaysia. Tel: 0060132034024. E-mail: gn11_phy021@student.usm.my

(Received 11 December 2014; revised 18 December 2014; accepted 13 January 2015)

The procedure for sample preparation involves several steps. Firstly, RBCs were diluted in phosphate-buffered saline (PBS), to obtain the maximum concentration measurable at maximum absorption. The maximum peak of RBCs was near 2.0 at 577 nm. To test the applicability of SiNP-encapsulated MB in for PDT, the diluted RBCs were mixed with the five different concentrations of MB-SiNPs and exposed to light source (~8.92 mW/cm^2 arc lamp, with 40 cm between the sample and the light source) at different times (0, 10, 20, 30, 40, 50, 60, 70, 80 and 90 min). The efficacy of naked MB was also tested, using five different concentrations of MB (final concentrations of 25.0, 12.5, 6.3, 3.1, and 1.6 μM) under light exposure of different times (0, 20, 40, 60, 80, 100, 120, 140, 160, and 180 min). Comparative analysis was performed between the results for encapsulated MB-SiNPs and naked MB. The changes in the absorption spectra of all samples were studied. The relationship between the concentration of the PS and the time needed to destroy 50% of the RBCs (t_{50}) (half-life time) was also analyzed (Al-Akhras et al. 2013). The dependence of the delayed photohemolysis on the concentration of the PS could then be expressed empirically by the following equations (Al-Akhras et al. 2013):

$$1/t_{50} = k.C^{(p)} \quad (1)$$

$$\mathrm{Ln}(1/t_{50}) = \mathrm{Ln}(k) + p\,\mathrm{Ln}(C) \quad (2)$$

where k is constant, C is the PS concentration, and p is the power-dependent parameter.

Results

The average size of SiNP-encapsulated MB was measured using DLS, and was found to be approximately 11.62 nm, as shown in Figure 1.

Effect of naked and encapsulated MB on RBCs

The effect of different concentrations of naked and encapsulated MB on RBC spectra in the visible range is shown in Figures 2–5. As shown in Figure 2a and b, the encapsulated MB at 2.5 μM concentration needed only about 20 min to destroy half of the spent RBCs, compared to the naked MB

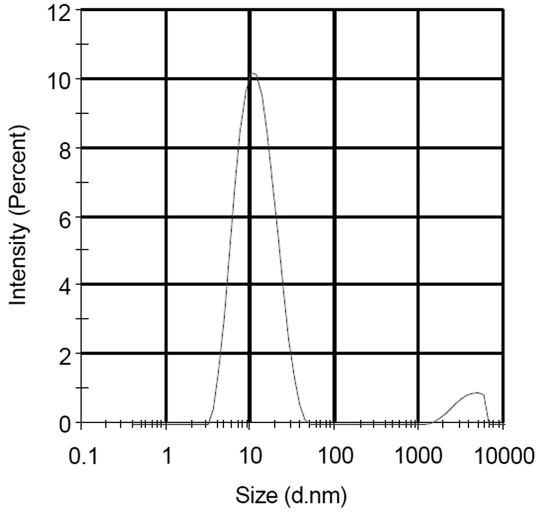

Figure 1. Size distribution of SiNP-encapsulated MB.

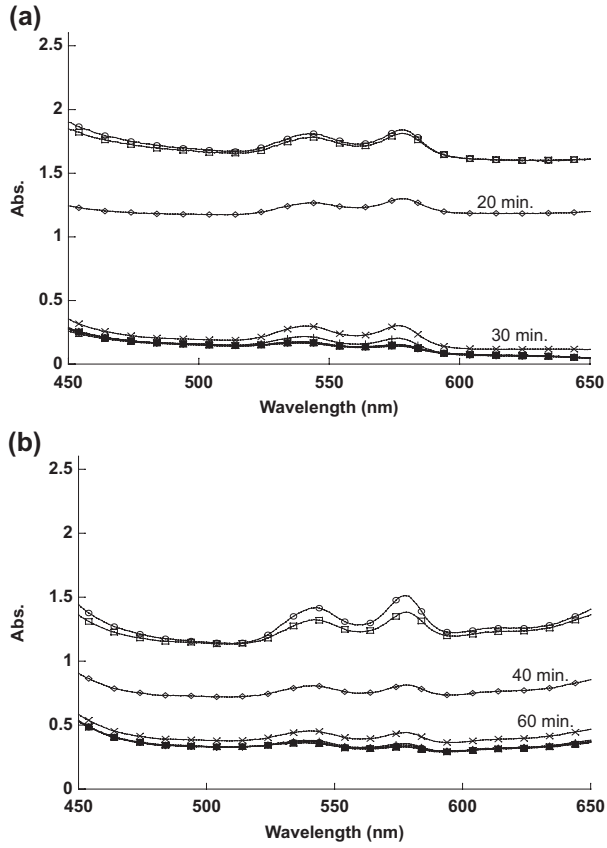

Figure 2. Changes in RBC spectra during irradiation with: (a) Encapsulated MB (2.50 μM), and (b) Naked MB (25.0 μM).

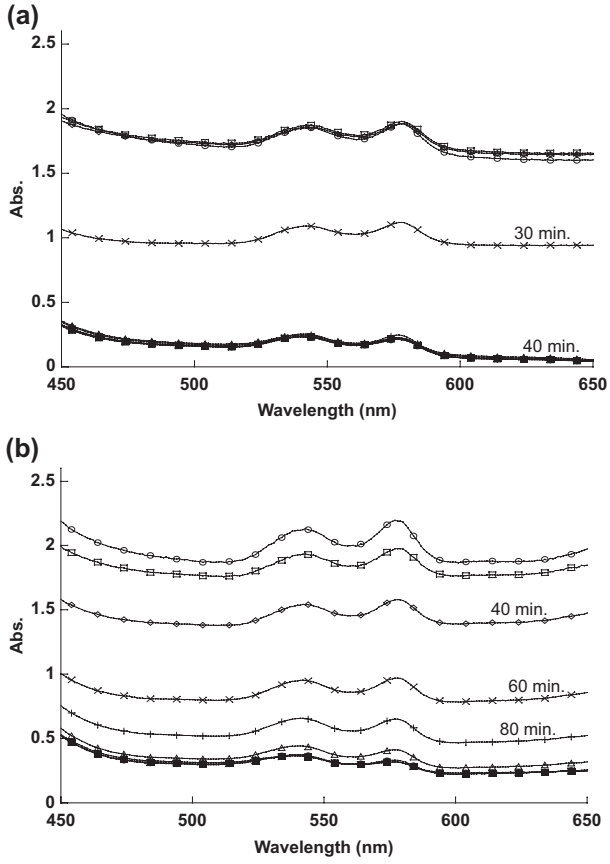

Figure 3. Changes in RBC spectra during irradiation with: (a) Encapsulated MB (1.25 μM), and (b) Naked MB (12.5 μM).

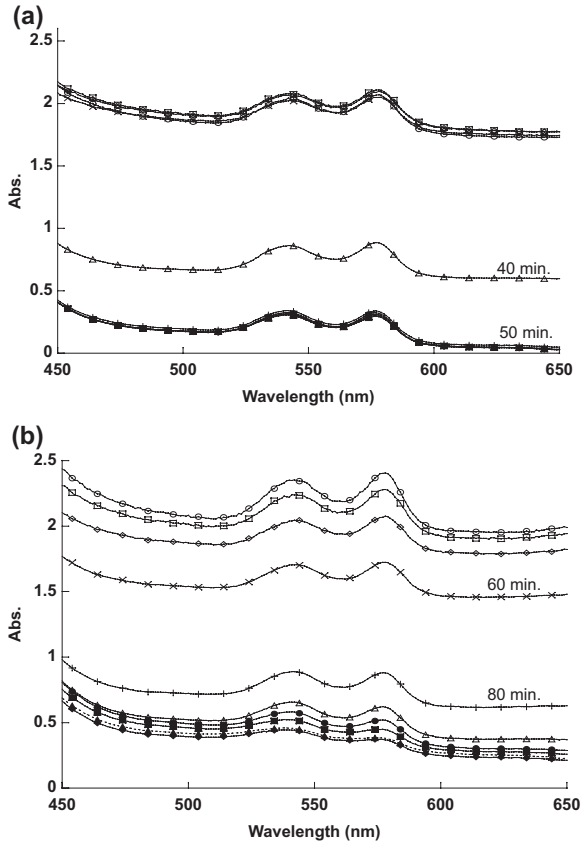

Figure 4. Changes in RBC spectra during irradiation with: (a) Encapsulated MB (0.63 μM), and (b) Naked MB (6.3 μM).

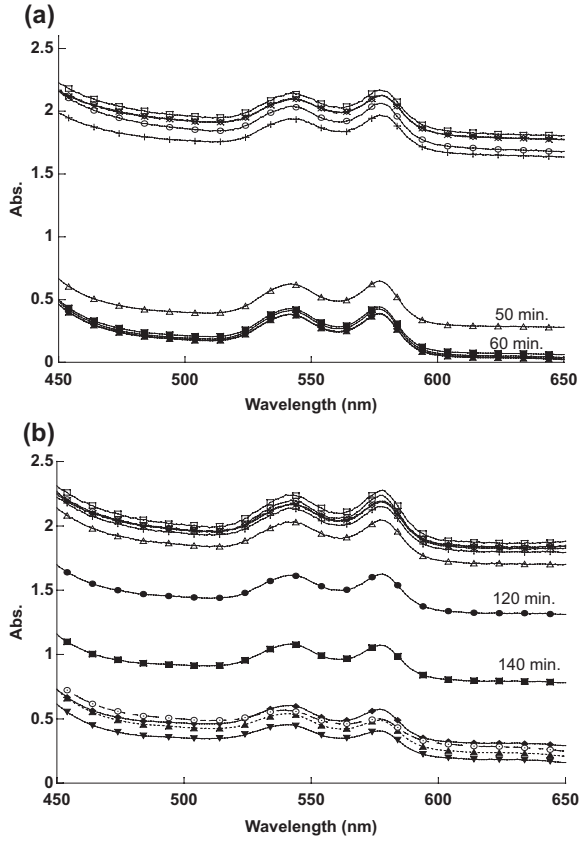

Figure 5. Changes in RBC spectra during irradiation with: (a) Encapsulated MB (0.31 μM), and (b) Naked MB (3.1 μM).

at 25.0 μM, which required approximately 40 min to reach similar efficacy.

At lower concentrations, the encapsulated MB, at a concentration of 1.25 μM, needed only about 30 min to destroy half of the RBCs, compared to the naked MB at 12.5 μM, which required approximately 60 min to destroy half of the RBCs, as shown in Figure 3a and b.

For Figure 4a and b, the encapsulated MB, at a concentration of 0.63 μM, needed less than 40 min to destroy half of the RBCs, compared to the naked MB at 6.3 μM, which required more than 60 min to destroy same number of RBCs.

Encapsulated MB, at a concentration of 0.31 μM, required about 40 min to destroy half of the RBCs, while naked MB, at the same concentration of 3.1 μM, required about 130 min to achieve the effect, as shown in Figure 5a and b respectively.

As shown in Figure 6a and b, the encapsulated MB, at 0.16 μM concentration, needed approximately 50 min to destroy half of the RBCs, compared to the naked MB, at 1.6 μM, that required more than 160 min to destroy half of the RBCs.

Fractional hemolysis and half-life time of RBCs with MB

Figure 7 shows a decrease in the maximum peak of RBCs after exposure to five different concentrations of naked and encapsulated MB. The maximum peaks for all different concentrations of naked and encapsulated MB were decreased after sufficient exposure time, as shown in Figure 7.

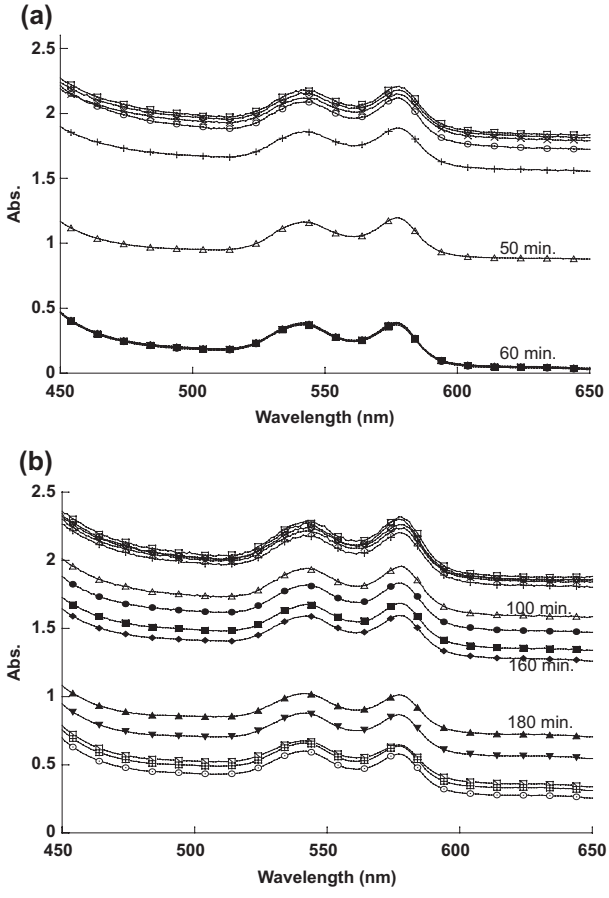

Figure 6. Changes in RBC spectra during irradiation with: (a) Encapsulated MB (0.16 μM), and (b) Naked MB (1.6 μM).

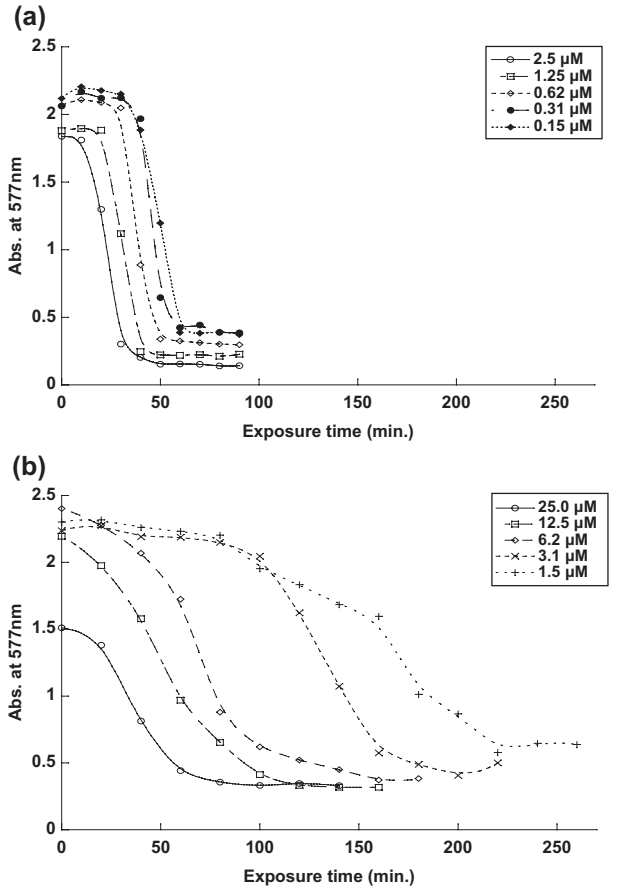

Figure 7. The reduction of the maximum peak for all samples: (a) Encapsulated MB, and (b) Naked MB.

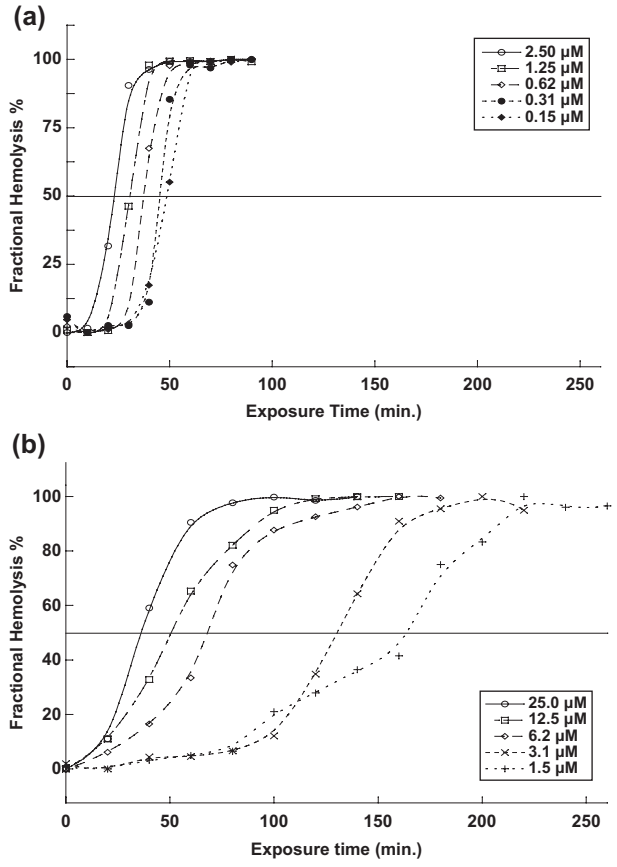

Figure 8. The normalization of maximum peak for all samples: (a) Encapsulated MB and (b) Naked MB.

The percentage of fractional hemolysis of RBCs during the exposure time is shown in Figure 8. At 50% of the fractional hemolysis, the half-life time (t_{50}) of RBCs can be measured. The half-life time (t_{50}) of RBCs was found to decrease with an increase in the concentration of naked and encapsulated MB.

The equations [Eq. 2] that define the relationship between the concentration of naked and encapsulated MB, and t_{50} of the RBCs are $[\mathrm{Ln}(1/t50) = -3.4499 + 0.26552\ \mathrm{Ln}(C)]$, and $[\mathrm{Ln}(1/t50) = -5.3690 + 0.56896\ \mathrm{Ln}(C)]$, respectively (Al-Akhras et al. 2013), as shown in Figure 9. These equations can be used in future work, to predict the exposure time that is needed to destroy the RBCs for other different concentrations of naked and encapsulated MB.

Discussion

The observed decrease in the RBC spectra in Figures 2–6 is attributable to the $^1O_2$ produced following the exposure of MB to the light source. The $^1O_2$ ruptured the RBCs' membranes, resulting in the spread of hemoglobin in the sample, thus decreasing the absorption spectra. The efficacy of naked MB at ten times the concentration was then compared to that of encapsulated MB. It is evident from the results that SiNP-encapsulated MB has a relatively higher efficacy in destroying RBCs compared to naked MB, because the MB molecules, clustered together by the SiNP encapsulation,

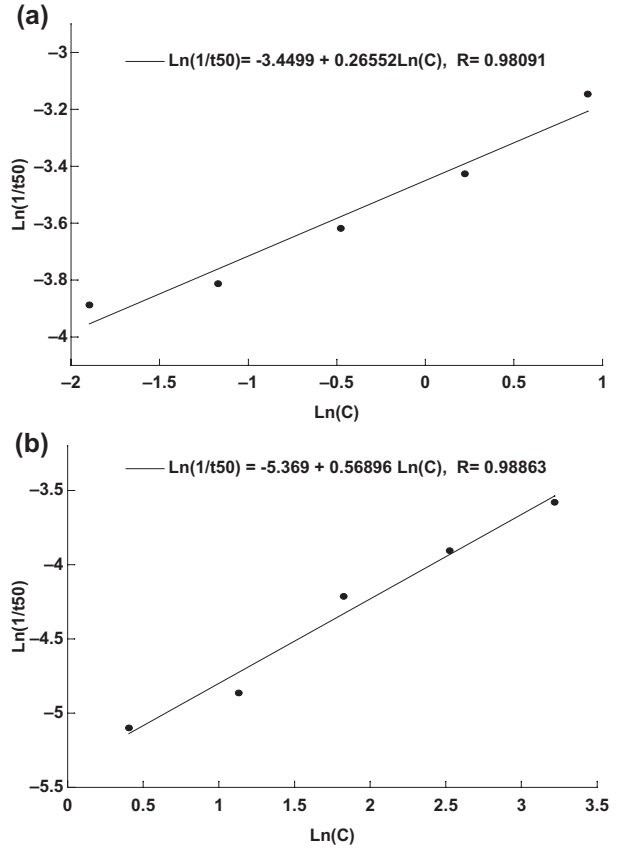

Figure 9. The relation between the half-life time of RBCs and the concentration of (a) Encapsulated MB, and (b) Naked MB.

cause high absorbance of light energy when in contact with RBCs.

The reason for the changes in the spectra, as shown in Figure 7, was the $^1O_2$ that was produced after exposing MB to the light source. The naked and encapsulated MB did not destroy the RBCs directly after exposure time, because they need to absorb sufficient energy from the light to produce the $^1O_2$. Singlet oxygen damaged the membrane of RBCs, thus spreading the hemoglobin in the outer liquid, and causing the reduction in the RBCs' absorption values. It is apparent from the results that RBCs were destroyed at less exposure time as the concentration of MB was increased.

When the concentration of MB was increased, the amount of $^1O_2$ produced also increased, thus destroying half of the RBCs faster, as shown in Figure 8. RBCs were destroyed faster when treated by encapsulated MB, because the encapsulated MB molecules absorbed high energy light compared to the naked MB molecules that spread in the sample.

From the results, it can be deduced that SiNP encapsulation allowed light to effectively penetrate through the membrane to reach the MB, which subsequently increased $^1O_2$ production and the destruction of RBCs. The efficacy of encapsulated MB in inducing RBC death was found to be comparably higher than that of naked MB, given that the rupturing of the RBCs required ten-fold a concentration of naked MB compared to that needed with encapsulated MB. This phenomenon is attributable to the fact that SiNP encapsulation is able to secure clusters of MB molecules that subsequently increase the absorbance of light energy. However, for naked MB, the molecules are distributed randomly in the solution, and their interaction with light are slower and dispersed, resulting in low absorbance. The relation derived between t_{50} and the concentration of naked MB and encapsulated MB can be applied in future studies, to calculate the most appropriate exposure time for the optimal concentration, without having to perform any experiments.

Declaration of interest

The authors report no declarations of interest. The authors alone are responsible for the content and writing of the paper.

References

Al-Akhras M-AH, Aljarrah K, Makhadmeh GN, Shorman A. 2013. Introducing the effect of chinese chlorella as a photosensitizing drug at different temperatures. J Mol Pharm Org Process Res. 1:1–4.

Bharali DJ, Klejbor I, Stachowiak EK, Dutta P, Roy I, Kaur N, et al. 2005. Organically modified silica nanoparticles: A nonviral vector for in vivo gene delivery and expression in the brain. Proc Natl Acad Sci USA. 102:11539–11544.

Chatterjee DK, Fong LS, Zhang Y. 2008. Nanoparticles in photodynamic therapy: An emerging paradigm. Adv Drug Deliv Rev. 60:1627–1637.

Deng T, Li JS, Jiang JH, Shen GL, Yu RQ. 2006. Preparation of Near-Ir fluorescent nanoparticles for fluorescence-anisotropy-based immunoagglutination assay in whole blood. Adv Funct Mater. 16:2147–2155.

He X, Wu X, Wang K, Shi B, Hai L. 2009. Methylene blue-encapsulated phosphonate-terminated silica nanoparticles for simultaneous *in vivo* imaging and photodynamic therapy. Biomaterials. 30: 5601–5609.

Kneuer C, Sameti M, Haltner EG, Schiestel T, Schirra H, Schmidt H, Lehr C-M. 2000. Silica nanoparticles modified with aminosilanes as carriers for plasmid DNA. Int J Pharm. 196:257–261.

Redmond RW, Gamlin JN. 1999. A compilation of singlet oxygen yields from biologically relevant molecules. Photochem Photobiol. 70:391–475.

Santra S, Yang H, Dutta D, Stanley JT, Holloway PH, Tan W, et al. 2004. TAT Conjugated, FITC doped silica nanoparticles for bioimaging applications. Chem Commun. 2810–2811.

Zhao Y, Sadtler B, Lin M, Hockerman GH, Wei A. 2004. Nanoprobe implantation into mammalian cells by cationic transfection. Chem Commun. 784–785.